Crystal Structure and NMR Investigation of the Serine Proteinase Inhibitor MR889, a Cyclic Thiolic Compound

Menico Rizzi,[a] Elena Casale,[a] Paolo Ascenzi,[b] Mauro Fasano,[c] Silvio Aime,[c] Concetta La Rosa,[d] Maurizio Luisetti[e] and Martino Bolognesi[a,f,*]

[a] *Dipartimento di Genetica e Microbiologia, Università di Pavia, Via Abbiategrasso 207, 27100 Pavia, Italy*
[b] *Dipartimento di Scienza e Tecnologia del Farmaco, Università di Torino, Via P. Giuria 9, 10125 Torino, Italy*
[c] *Dipartimento di Chimica Inorganica, Chimica Fisica e Chimica dei Materiali, Università di Torino, Via P. Giuria 7, 10125 Torino, Italy*
[d] *Medea Research, Via C. Pisacane 34/a, 20129 Milano, Italy*
[e] *Istituto di Tisiologia e Malattie Respiratorie, Università di Pavia, IRCCS Policlinico San Matteo, Via Taramelli 5, 27100 Pavia, Italy*
[f] *I.S.T., Gruppo Biostrutture, Università di Genova, Viale Benedetto XV 10, 16132 Genova, Italy*

The serine proteinase inhibitor *N*-(2-oxo-2,3,4,5-tetrahydro-3-thienyl)-2-(2-thenoylthio)propionamide (MR889) has been crystallised, and its three-dimensional structure studied by X-ray diffraction and by NMR techniques in solution and in the solid state. MR889 crystallises in the monoclinic space group $P2_1/n$ with cell constants a = 10.539(2), b = 9.647(5), c = 14.654(1) Å, β = 101.62(1)°; the asymmetric unit contains one molecule of MR889. The weighted crystallographic R factor for the refined structure is 0.044.

The solution structure of MR889 has been elucidated through the measurement of proton–proton and proton–carbon nuclear Overhauser enhancements. Measurement of the ^{13}C longitudinal relaxation times yields information about the dynamics of MR889 in dimethylsulfoxide solution. The comparison between solid and solution state ^{13}C NMR spectra allows an understanding of the quite different structures in the two states.

Proteases and their zymogens play a central role in several biological processes, spanning from digestion to key regulatory mechanisms such as coagulation and hormone release and also being recognized in many diseases.[1-3] Therefore, the possibility of selectively influencing enzyme activities by specific inhibitors appears of considerable interest in view of their potential therapeutic value as drugs.[2]

Serine proteinase activity can be modulated by protein enzyme inhibitors, as well as by low molecular weight synthetic molecules, such as the cyclic thiolic compound *N*-(2-oxo-2,3,4,5-tetrahydro-3-thienyl)-2-(2-thenoylthio)propionamide [MR889; see Fig. 1(*a*)] and *N*-(4-carboxy-2,3,4,5-tetrahydro-3-thienyl)-2-(2-thenoylthio)propionamide [YS3025, see Fig. 1(*b*)].[1-10] These acylating agents, which preferentially react with serine proteinases belonging to the chymotrypsin superfamily acting on non-cationic substrates[5-10] display apparent equilibrium dissociation constants ranging between 1 × 10^{-6} and 1 × 10^{-5} mol dm^{-3} for bovine α-chymotrypsin, human leukocyte- and porcine pancreatic-elastase.[5-10] The second-order combination rate constant and the first-order dissociation rate constant for the human leukocyte elastase: MR889 and YS3025 complex (de)stabilization are 2.4 × 10^3 dm^3 mol^{-1} s^{-1} and 3.0 × 10^{-3} s^{-1} respectively.[6,7] Moreover, MR889 inhibits the hydrolysis of insoluble elastin catalyzed by human leukocyte elastase, *i.e.* the cleavage of the physiological target of this serine proteinase.[6-8] These findings, together with the limited toxicity of MR889,[6] are prerequisites for the therapeutical application of these low molecular weight serine proteinase inhibitors.[2,6]

Finally, concerning the molecular mechanism of serine proteinases inhibition by MR889 and YS3025, Powers *et al.*[8] and Rizzi *et al.*[9] have shown that the MR889 and YS3025 acylenzyme adducts contain the thiophenecarbonyl moiety of the inhibitor covalently bound to the Ser195 OG atom [see Fig. 1(*c*)].

In view of the potential application of these compounds in the treatment of inflammatory and lung diseases, we have characterized the molecular structure of MR889, the parent molecule in this inhibitor family, by crystallographic and NMR investigation.

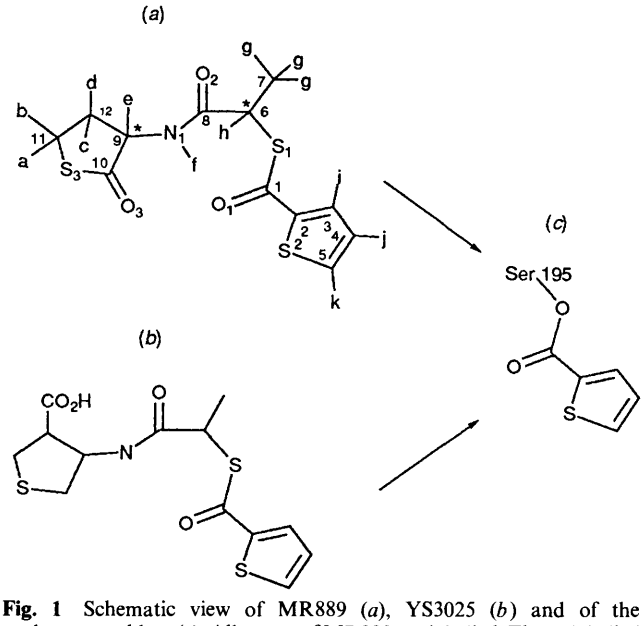

Fig. 1 Schematic view of MR889 (*a*), YS3025 (*b*) and of the acylenzyme adduct (*c*). All atoms of MR889 are labelled. The unlabelled oxygen atom in the acyl-enzyme is the proteinase Ser195 OG atom. The asterisks indicate the two centres of asymmetry [C(6) and C(9)] present in MR889 (*a*).

Experimental

MR889 was synthesized as described previously.[11] The molecule contains two centres of asymmetry [marked in Fig.

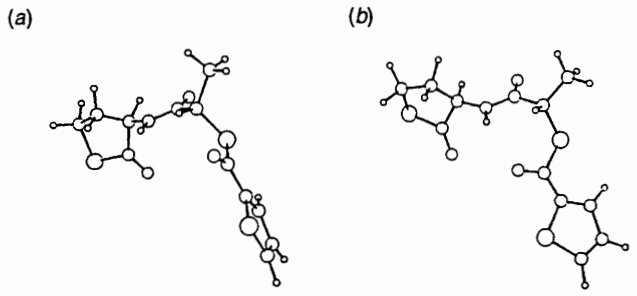

Fig. 2 Structure of MR889, as determined by X-ray diffraction (*a*) and by the solution NMR derived structural parameters (*b*)

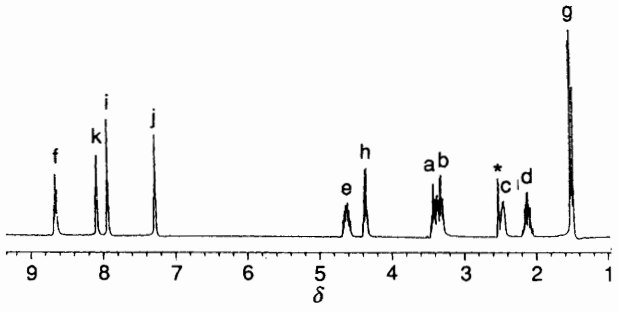

Fig. 3 ^{1}H NMR spectrum of a solution of MR889 in [$^2H_6$]DMSO. Labelling as in Fig. 1. The FID was apodized with an exponential window using a negative line broadening of −0.05 Hz to improve the resolution. The flip angle used was 45° (6.5 μs); the number of scans was 36 with a recycle delay of 5 s. The asterisk indicates the solvent signal.

1(*a*) with asterisks], giving rise to two pairs of enantiomers, present in a 1 : 1 ratio in the samples used.[6,11] All the products were purchased from Merck AG (Darmstadt, Germany). All chemicals were of analytical grade and used without further purification.

MR889 crystals were grown in a saturated methanol solution by slow evaporation. Unit cell parameters and intensity data were obtained on an Enraf–Nonius CAD-4 diffractometer with graphite monochromated Cu-Kα radiation (λ = 1.541 84 Å). The size of the crystal used was 0.5 × 0.5 × 0.3 mm. Cell dimensions were determined from 25 centred reflections monitored in the range 25° < θ < 45°. The space group was evaluated from systematic extinctions and intensity statistics. Diffracted intensities were measured up to sin θ/λ = 0.6083 Å^{-1}, for a total of 2958 reflections, with the $\omega/2\theta$ scan method. Control of crystal orientation and decay was performed periodically using three selected reflections, which showed no significant decay of the diffracted intensities. Lorentz polarisation and empirical absorption correction[12] were applied. The value of the R_{sym} factor for the 259 equivalent reflections collected in the *hk*0 zone was 0.039 [$R_{sym} = (\Sigma_i||I_i| - |I||)/(\Sigma_i|I|)$, where I_i is the intensity recorded in the *i*-th measurement of a reflection whose average intensity is I, and the sum is over all the equivalent reflections].

The structure was solved by direct methods (MULTAN80).[13] Positions of all non hydrogen atoms were revealed from the E map using the highest CFOM (3.00). Refinement was achieved by full-matrix least-squares methods. Non-hydrogen atoms were refined anisotropically. Hydrogen atoms were placed in idealized positions and constrained to have a C–H bond length of 0.95 Å; their thermal parameters were set at a value equivalent to the isotropic thermal parameter of the nearest bonded atom. The refinement converged at a value of the conventional crystallographic *R*-factor of 0.078, while for the 172 parameters and 2067 observed reflections the weighted *R*-factor was 0.044. Atomic scattering factors with anomalous dispersion coefficient were taken from the International Tables for X-ray crystallography.[14] All calculations were performed on a MICROVAX-3100 computer; the atomic coordinates, bond distances and angles have been deposited at CCDC.* A view of the asymmetric unit is reported in Fig. 2(*a*).

The solutions for NMR experiments were prepared in [$^2H_6$]-DMSO. 1D and 2D NMR solution spectra were recorded at 298 K on a JEOL EX-400 Fourier Transform NMR spectrometer operating at a magnetic field strength of 9.4 T.

The proton–proton correlation spectrum was obtained with the conventional DQF–COSY[15] pulse sequence. The proton–carbon direct and long-range correlation spectra were obtained with inverse detection techniques[16,17] (HMQC and HMBC respectively).

For the evaluation of the proton–proton distances, three NOESY spectra using different mixing time (100, 200 and 500 ms) were recorded.[18] Data processing, including surface fitting for the cross-peak volume calculation, was conducted on a DEC-2100® RISC-Workstation with the NMRi® program package.[19]

The ^{13}C NMR spectrum of the solid MR889 sample was recorded at 298 K on a JEOL GX-270 FT NMR spectrometer, operating at a magnetic field strength of 6.4 T (^{13}C Larmor frequency of 67.80 MHz), under Cross-polarization Magic Angle Spinning (CPMAS) mode.[20] The sample (about 0.6 g) was placed in a zirconia rotor (7 mm o.d.) and spun at a rate of 4600 Hz. The contact time in the cross polarization experiment was 7500 μs. The recycle time was 10 s; the signal was filtered with an exponential function (line broadening = 10 Hz) to improve the S/N ratio.

Distances and angles obtained from NMR data were refined with the MM2 Force Field,[21] starting from the crystal structure.

Results and Discussion

The serine proteinase synthetic inhibitor MR889 was crystallized in the monoclinic space group $P2_1/n$, with unit cell constants a = 10.539(2), b = 9.647(5), c = 14.654(1) Å, β = 101.62(1)°. One MR889 molecule is contained in the asymmetric unit.

The crystal structure of the synthetic inhibitor MR889 was solved by direct methods, and refined to a weighted crystallographic factor of 0.044 [see Fig. 2(*a*)]. All bond lengths and angles conform to their standard values;[14] a close inspection of these values in the carbonyl–thiophene part of MR889 shows that delocalization of the π electrons is occurring, as indicated by the short length of the C(1)–C(2) bond. The S(2) atom of the thiophene ring is in *trans* position with respect to the S(1) atom of the thioester bond. In the crystal lattice the molecule is hydrogen-bonded through the N(1)-H amido group to the O(2) atom of the amido group of a neighbouring symmetry related molecule, the N • • • O distance being 2.986(6) Å. Moreover, the two chiral centres observed in the crystal structure display *R*,*S* and *S*,*R* configurations.

As previously established,[11] MR889 is sparingly soluble in most solvents whereas it shows a very high solubility in DMSO, which was then chosen to prepare the solutions for NMR solution studies. The ^{1}H NMR spectrum is reported in Fig. 3. All the resonances were unambiguously assigned through a two-dimensional DQF–COSY[15] experiment. The multiplicity of some of the ^{1}H resonances are further complicated by an additional splitting associated to the presence of two chiral centres [C(6) and C(9)] which make these resonances diastereotopic and no longer anisochronous from the NMR point

* Details of the deposition scheme can be found in issue 1, *J. Chem. Soc., Perkin Trans. 2*, 1993.

Table 1 Data for MR889 from NMR results

H–H	Distance/Å
a–c	2.44
b–c	3.09
d–a	2.66
d–b	2.48
e–d	2.48
e–c	3.10
e–f	2.34
Dihedral angle	**(°)**
H_a–C(11)–C(12)–H_c	46
H_a–C(11)–C(12)–H_d	73
H_b–C(11)–C(12)–H_c	165
H_b–C(11)–C(12)–H_d	47
H_c–C(12)–C(9)–H_e	163
H_d–C(12)–C(9)–H_e	44
H_e–C(9)–N(1)–H_f	45

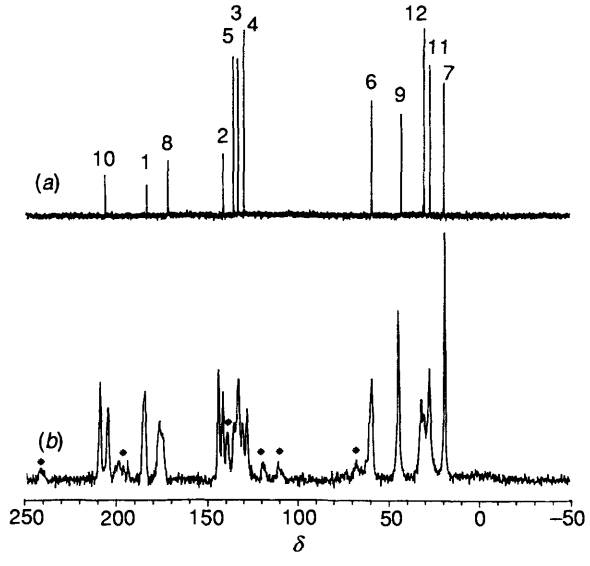

Fig. 4 ^{13}C NMR broadband-proton-decoupled spectra of MR889; (*a*) solution spectrum in [$^2H_6$]DMSO; (*b*) solid-state, cross polarisation, magic angle spinning spectrum; asterisks indicate the spinning sidebands. Labelling as in Fig. 1.

of view. The ^1H–^1H coupling pattern was analysed on the basis of the modified Karplus relationship,[22] which provided a number of dihedral angles.

As the experimental temperature was increased from 300 to 373 K, only the N–H resonance at 8.65 ppm was affected, showing an upfield shift of 0.37 ppm. Clearly, the observed behaviour is indicative of a hydrogen bond involving the N–H amido moiety. Three cases may be envisaged thus, (i) an intermolecular N–H - - O=C(8) bond between two MR889 molecules as observed in the crystalline state; (ii) an intramolecular N–H - - O=C(1) interaction which would provide a structure quite different from that found in the solid state; and (iii) an intermolecular interaction between the N–H hydrogen and the solvent DMSO molecules. Case (i) is ruled out by the observation that the N–H chemical shift is concentration independent. It is more difficult to distinguish between case (ii) and (iii). It was shown earlier[23] that it is possible to distinguish between amide resonances involved in intramolecular or solute–solvent hydrogen bond formation by looking at the magnitude of the shift/temperature coefficient. Large negative coefficients (from −0.005 to −0.008 ppm K^{-1}) indicated interaction with the solvent molecules, whereas the intramolecular hydrogen bond resulted in quite small either negative or positive coefficients (±0.001 ppm K^{-1}). We observe an upfield temperature dependent shift of 0.0051 ppm K^{-1} which supports the occurrence of case (iii).

Some further structural details were obtained by measuring proton–proton NOE in a 2D NOESY experiment. The relatively small size of the MR889 molecule allows a fast reorientational molecular motion which limits the detection of NOEs to those inside the aliphatic ring.[18,24] From the ratio of diagonal and cross peaks volumes (a_{AA} and a_{AB} in the following equation) of the five resonances, we may estimate the interproton distance r_{AB} for each mixing time (τ_{mix}) value[25] [see eqn. (1), where $q = 0.1\ \gamma^4h^4(\mu_0/4\pi)^4$]. The advantage of this

$$r_{AB} = \frac{-2q\tau_{mix}}{\ln\dfrac{a_{AA} + a_{AB}}{a_{AA} - a_{AB}}} \times \frac{6\tau_c}{(1 + 4\omega^2\tau_c^2)} \qquad (1)$$

approach is that we need only a single NOESY experiment, with a short mixing time, so that no spin-diffusion occurs, but not too short, so that cross peaks are sufficiently intense.

On the basis of the calculated dihedral angles, interproton distances and, in the absence of the intramolecular hydrogen bonds, the solution structure was refined using the molecular mechanics MM2 Force Field[21] [Fig. 2(*b*)]. The refined values of the interproton distances and of the dihedral angles are reported in Table 1.

Further support for this picture arises from comparison between solution and solid state ^{13}C NMR spectra (Fig. 4). The assignment of the ^{13}C resonances was performed on the solution spectrum on the basis of several observations including DEPT, ^{13}C–^1H and ^{13}C–^{13}C coupling patterns in 1D experiments as well as in proton detected 2D correlation experiments (HMQC and HMBC). The number of ^{13}C resonances observed in the solid-state spectrum under Cross Polarisation Magic Angle Spinning (CPMAS) mode is higher than the corresponding solution spectrum since we may expect to have the formation of racemic and enantiomerically pure crystallites.

Intermolecular interactions in the two types of crystals are diastereotopic and in some cases resulted in a substantial difference in their isotropic chemical shifts. Now, on comparing the isotropic solid-state chemical shifts with the solution shifts we noted a fairly good correspondence with most of the resonances but C(8) which shows an upfield shift on going from the solid to the solution state. This behaviour reflects the fact that this C=O group in the crystal structure is forming a hydrogen bond with the amido hydrogen of a neighbouring molecule which breaks down in the solution state. Such an upfield shift following the hydrogen bond break-up is well documented for C=O groups.[26]

Finally, we undertook the measurement of relaxation times and NOE of ^{13}C resonances of MR889 to get an overview of the molecular dynamics of the molecule in DMSO solution. The relaxation rates R_1 ($=1/T_1$) measured at the magnetic field strength of 9.4 T are reported in Table 2. As expected, the protonated carbon resonances show higher relaxation rates whereas the carbonyl and quaternary carbon resonances possess much longer relaxation times. From the measurement of the NOE for each ^{13}C resonance we evaluate the dipolar contribution to the overall relaxation rate, eqn. (2).

$$R_1^{DD} = \text{NOE} \times R_1 \qquad (2)$$

Now, by introducing the standard values for ^{13}C–^1H distances (r) in sp^2 and sp^3 C–H fragments[14] we get an estimate of the effective correlation time characterising the

Table 2 Chemical shifts, relaxation rates, NOEs, dipolar relaxation rates and reorientational correlation times of carbon nuclei in MR889

C	δ	R_1 (9.4 T)	NOE	R_1^{DD}	τ_c/ps
1	182.2	0.163	—	—	78
2	140.7	0.100	0.20	—	67
3	132.0	1.63	1.20	0.83	41
4	128.7	1.89	1.39	1.15	57
5	134.6	2.42	1.47	1.64	81
6	58.5	1.95	1.29	0.95	47
7	19.0	1.73	1.90	1.49	25
8	170.6	0.228	0.33	—	73
9	42.6	2.11	1.52	1.78	87
10	204.8	0.148	—	—	70
11	26.9	3.19	1.99	2.63	65
12	30.0	2.88	1.99	2.78	68

modulation of the C–H dipolar interaction for each protonated carbon, eqn. (3).

$$\tau_{eff} = \frac{R_1^{DD} r^6}{\gamma_H^2 \gamma_C^2 \hbar^2} \quad (3)$$

For the non-protonated C(1), C(2), C(8) and C(10) resonances we got an estimation of τ_c by assuming that the dominant relaxation process occurs through the modulation of their Chemical Shift Anisotropies (CSA). For C(2) and C(8) resonances which show sizeable NOEs R_1^{CSA} is determined by subtracting R_1^{DD} from the measured R_1 values. Then, by introducing in eqn. (4), CSA values of 200 ppm for C(1), C(8),

$$R_1^{CSA} = 2/15\gamma^2 \, CSA^2 \, B_0^2 \tau_c \quad (4)$$

C(10) carbonyl resonances and of 150 ppm for the C(2) aromatic resonance we obtained the τ_c parameter for these carbons as well.

The values reported in Table 2 show that the tumbling of the molecule in DMSO solution is essentially isotropic, and only the atoms along the rotation axes of the cyclic groups [C(5) and C(9)] possess a slightly longer correlation time. The methyl carbon shows the shortest τ_c value as the result of a superposition of the internal rotation to the overall molecular tumbling.

The present study brings information on the solid state and solution structure of a synthetic serine proteinase cyclic thiolic inhibitor. The experimental evidences reported show that the molecular structures and conformations of MR889 in the two states are comparable. Indeed from the viewpoint of biological activity, both observed conformations display a fully accessible electrophile C(1) atom, which can be properly reached by the target enzyme Ser195 OG atom, at the onset of the acylation reaction.

Absence of intramolecular interactions, and thus of more 'closed' conformations for MR889, is also in keeping with its prompt reaction at the active site of enzymes from the chymotrypsin superfamily.[9,10]

Acknowledgements

This study was partly supported by grants from the Italian Ministry of University, Scientific Research and Technology (MURST), as well as of the Italian National Research Council (CNR), target oriented projects '*Biotecnologie e Biostrumentazione*' and '*Chimica Fine II*'.

References

1 H. Hörn and A. Heidland, *Proteases: Potential Role in Health and Diseases*, Plenum Press, New York, 1982.
2 A. J. Barrett and G. Salvesen (eds.), *Proteinase Inhibitors*, Elsevier, Amsterdam, 1986.
3 D. D. Cunningham and G. L. Long (eds.), *Proteinases in Biological Control and Biotechnology*, Alan R. Liss Inc., New York, 1988.
4 T. Hutchens (ed.), *Protein Recognition of Immobilized Ligands*, Alan R. Liss Inc., New York, 1989.
5 M. Luisetti, P. D. Piccioni, M. Donnini, V. Peona, E. Pozzi and C. Grassi, *Biochem. Biophys. Res. Commun.*, 1989, **165**, 568.
6 A. Baici, R. Pelloso and D. Horler, *Biochem. Pharmacol.*, 1990, **39**, 919.
7 A. Baici, in *Biochemistry of Pulmonary Emphysema*, eds. G. Grassi, J. Travis, L. Casali and M. Luisetti, Springer Verlag, Berlin, and Bi & Gi Publishers, Verona, 1992, p. 81.
8 J. C. Powers, C. M. Kam, H. Hori, J. Oleksyszyn and E. F. Meyer, Jr., in *Biochemistry of Pulmonary Emphysema*, eds. G. Grassi, J. Travis, L. Casali and M. Luisetti, Springer Verlag, Berlin, and Bi & Gi Publishers, Verona, 1992, p. 123.
9 M. Rizzi, E. Casale, A. Coda, C. La Rosa, P. Ascenzi, M. Luisetti and M. Bolognesi, *Biochemistry Int.*, 1992, **28**, 385.
10 K. Djinovic, M. Rizzi, M. Fasano, M. Luisetti, C. La Rosa, P. Ascenzi and M. Bolognesi, *Biochem. Biophys. Res. Commun*, 1993, **193**, 32.
11 EP 0 120 534/1987, USP 4 481 212/1984.
12 A. C. T. North, D. C. Phillips and F. S. Mathews, *Acta Crystallogr., Sect. A*, 1968, **24**, 351.
13 P. Main, S. J. Fiske, S. E. Hull, L. Lessinger, G. Germain, J. P. Declercq and M. M. Woolfson, MULTAN 80, a system of computer programs for the automatic solution of crystal structures from X-ray diffraction data, University of York, England and of Louvain, Belgium, 1980.
14 *International Tables for X-Ray Crystallography*, vol. IV, Kynoch Press, Birmingham, 1974.
15 M. Rance, O. W. Sørensen, G. Bodenhausen, G. Wagner, R. R. Ernst and K. Wüthrich, *Biochem. Biophys. Res. Commun.*, 1986, **117**, 479.
16 L. Müller, *J. Am. Chem. Soc.*, 1979, **101**, 4481.
17 A. Bax and M. F. Summers, *J. Am. Chem. Soc.*, 1986, **108**, 2093.
18 D. Neuhaus and M. P. Williamson, *The Nuclear Overhauser Effect in Structural and Conformational Analysis*, VCH Publishers, New York, 1989.
19 New Methods Research, Inc., 6035 Corporate Dr., East Syracuse, NY 13057-1016.
20 C. A. Fyfe, *Solid State NMR for Chemists*, C.F.C. Press, Guelph, Ontario, 1983.
21 N. L. Allinger and Y. H. Yuh, QCPE Program 395, Bloomington, Indiana, 1981.
22 C. A. G. Haasnoot, F. A. A. M. de Leeuw, H. P. M. de Leeuw and C. Altona, *Recl. Trav. Chim. Pays-Bas*, 1979, **98**, 576.
23 N. G. Kumar and D. W. Urry, *Biochemistry*, 1973, **12**, 4392.
24 M. Reggelin, H. Hoffmann, M. Köck and D. F. Mierke, *J. Am. Chem. Soc.*, 1992, **114**, 3272.
25 G. Esposito and A. Pastore, *J. Magn. Reson.*, 1988, **76**, 331.
26 N. Asakawa, S. Kuroki, H. Kurosu, I. Ando, A. Shoji and T. Ozaki, *J. Am. Chem. Soc.*, 1992, **114**, 3261.

Paper 3/02314A
Received 22*nd April* 1993
Accepted 2*nd June* 1993